

Effect of field-dependent core size on reversible magnetization of high- κ superconductors

V. G. Kogan, R. Prozorov,* S. L. Bud'ko, and P. C. Canfield

Ames Laboratory—DOE and Department of Physics and Astronomy, Iowa State University, Ames, Iowa 50011, USA

J. R. Thompson

*Materials Science and Technology Division, ORNL, Oak Ridge, Tennessee 37831, USA
and Department of Physics, University of Tennessee, Knoxville, Tennessee 3796-1200, USA*

J. Karpinski and N. D. Zhigadlo

Solid State Physics Laboratory, ETH, 8093 Zurich, Switzerland

P. Miranović

Department of Physics, University of Montenegro, 81000 Podgorica, Serbia and Montenegro

(Received 21 June 2006; revised manuscript received 11 September 2006; published 15 November 2006)

The field dependence of the vortex core size $\xi(B)$ is incorporated in the London model, in order to describe reversible magnetization $M(B, T)$ for a number of materials with large Ginzburg-Landau parameter κ . The dependence $\xi(B)$ is directly related to deviations in $M(\ln B)$ from linear behavior prescribed by the standard London model. A simple method to extract $\xi(B)$ from the magnetization data is proposed. For most materials examined, $\xi(B)$ so obtained decreases with increasing field and is in qualitative agreement both with behavior extracted from μ SR and small-angle neutron-scattering data and with that predicted theoretically.

DOI: [10.1103/PhysRevB.74.184521](https://doi.org/10.1103/PhysRevB.74.184521)

PACS number(s): 74.50.+r, 74.78.Fk

I. INTRODUCTION

Despite its simplicity, the London approach is a powerful tool in describing magnetic properties of the mixed state. In fact, short of the full-blown microscopic theory, it is the only method available for low temperatures. The approach is based on the London equation,

$$h - \lambda^2 \nabla^2 h = \phi_0 \sum_n \delta(\mathbf{r} - \mathbf{r}_n), \quad (1)$$

where $h(\mathbf{r})$ is the magnetic field, λ is the penetration depth (a temperature-dependent *constant* in uniform samples), ϕ_0 is the flux quantum, and \mathbf{r}_n are vortex positions. For simplicity, the equation is written for isotropic materials. This approach fails at distances of the order of the coherence length ξ ; still, in materials with $\kappa = \lambda/\xi \gg 1$, there is a broad domain of intermediate fields $\phi_0/\lambda^2 \ll H \ll \phi_0/\xi^2$ where the complexity of the vortex core contributions to the total energy can be disregarded and the London approach suffices for the description of macroscopic magnetic properties.

As far as the equilibrium properties of the flux-line lattice are concerned, the pivotal point is the expression for the free energy

$$\tilde{F} = F - \frac{B^2}{8\pi} = \frac{\phi_0 B}{32\pi^2 \lambda^2} \ln \frac{e\eta H_{c2}}{B}. \quad (2)$$

The right-hand side here is the interaction energy of vortices forming a periodic lattice; B is the magnetic induction. This expression is obtained by transforming the sum of pairwise interactions of vortices to a sum over the reciprocal lattice, see, e.g., Ref. 1. The sum (or the integral over the reciprocal plane \mathbf{k}) is logarithmically divergent so that a cutoff at $k \sim 1/\xi \sim 1/\rho_c$ is needed (ρ_c is the size of the vortex core). This yields $\ln(\phi_0/2\pi\xi^2 B)$ at the right-hand side of Eq. (2).

The parameter η of the order unity is commonly introduced to account for uncertainty of the cutoff (along with the uncertainty in the lower limit of the integral of the order of inverse intervortex spacing $\sim \sqrt{B/\phi_0}$; $e=2.718\dots$ appears in Eq. (2) for the convenience of not having it in the expression for the magnetization. Again, the energy in the form of Eq. (2) holds in intermediate fields $H_{c1} \ll H \ll H_{c2}$, the domain existing only in materials with large Ginzburg-Landau parameter κ (H_{c1} and H_{c2} are the lower and upper critical fields). Hence, although the length ξ (or the core size ρ_c) does not appear in the London equation (1), it enters the energy expression (2) through the cutoff and therefore affects, presumably weakly, macroscopic quantities such as the magnetization and other properties of the mixed state.

Significant effort has recently been put in studies of the vortex core size ρ_c ; see the review by Sonier and references therein.² Notably, whatever definition of ρ_c is adopted, the low temperature ρ_c (extracted from the μ SR data, see Refs. 2 and 3) decreases with increasing applied magnetic field in a number of materials such as NbSe₂, V₃Si, LuNi₂B₂C, YBa₂Cu₃O_{7- δ} , and CeRu₂; their physical characteristics have little to do with one other, except that all of them have a large GL parameter $\kappa = \lambda/\xi$ and exhibit large regions of reversible magnetic behavior. One can add to this list a heavy fermion compound CeCoIn₅, for which the interpretation of small-angle neutron-scattering data (SANS) requires a similar behavior of the coherence length.⁴ The dependencies $\rho_c(B)$ for all tested materials are qualitatively similar: when the field increases toward H_{c2} , $\rho_c(B)$ decreases roughly as $1/\sqrt{B}$. In other words, in large fields ρ_c is roughly proportional to the intervortex spacing.

A few qualitative reasons for the core shrinking with increasing field have been discussed in literature; see the review.² Perhaps the simplest defines the core boundary as a

position where the divergent London current $c\phi_0/8\pi^2\lambda^2r$ of an isolated vortex reaches the depairing value, i.e., as $r\sim\xi$. In the mixed state, neighboring vortices suppress the circulating current by contributing currents of the opposite direction. Hence, the depairing value is reached at a shorter distance from the vortex center, and consequently, ρ_c should decrease with increasing field.

The vortex core size ρ_c is of the order of the coherence length ξ and, in fact, it is often identified with $\xi(T)$. Strictly speaking, the latter is defined only at the upper critical field: $H_{c2}(T)=\phi_0/2\pi\xi^2$. Nevertheless, the length ξ is used to describe the mixed state at fields not necessarily close to H_{c2} . The question of possible field dependence of ξ has been considered by one of us for the isotropic case.⁵ It was shown that in the dirty limit one can use $\xi=(\phi_0/2\pi H_{c2})^{1/2}$ at any field within the mixed phase; the same is true near the critical temperature T_c for any scattering strength. However, in general, when the field is reduced below H_{c2} , the value of $\xi(B)$ increases, an effect that is profound in clean materials at low temperatures. Calculations of Ref. 6 are in accord with the μ SR results cited above. In the following, we denote as ξ_{c2} the value of $\xi(B)$ at $B=H_{c2}$ to stress that in general $\xi(B)\neq\xi_{c2}$ for $B<H_{c2}$.

Another common theoretical definition of ρ_c is based on the slope of the order parameter $\Delta(r)$ at the vortex axis $r=0$, normalized either to its value $\Delta(\infty)$ far from the single vortex or to the value of $\Delta(a/2)$ half way to the nearest neighbor in the mixed state: $1/\rho_c=\Delta'(0)/\Delta(a/2)$. Recent microscopic calculations of this quantity by Miranović *et al.* showed a variety of field-dependent behaviors of ρ_c at low temperatures depending on the scattering strength.⁷ In particular, this work suggests that $\rho_c(B)$ may have a minimum which, however, has not been seen in μ SR experiments. There are many different ways to define ρ_c customized for different experimental or theoretical needs (see, e.g., the discussion in Ref. 6). For the purpose of this paper, these differences are irrelevant and we use the terms $\rho_c(T, B)$ and $\xi(T, B)$ as the same.

In the following we provide experimental data for the field dependence of the reversible magnetization for a single crystal $\text{YNi}_2\text{B}_2\text{C}$ in a broad temperature region to demonstrate the known fact: the data cannot be described by the standard London model. We then derive a closed-form expression for the cutoff $\xi(B)$ needed to represent correctly the data $M(B)$ with the help of the London model. We show that $\xi(B)$ so chosen is qualitatively consistent with the field dependence of ξ recorded by μ SR and discussed theoretically. Finally, we demonstrate that the new model generates a consistent description of the magnetization data for a number of unrelated materials with large κ . The goal of this paper is to demonstrate that $\xi(B)$ can be in principle extracted from the magnetization data, a less demanding experimental procedure as compared to μ SR or SANS. Within our approach, *the London penetration depth is field independent*, whereas the field dependence of ξ alone suffices to explain the data.

II. EXPERIMENTAL ASPECTS

A. Sample preparation

For experimental studies, single-crystal samples of the highest available quality were selected, in order to eliminate

extrinsic impurity effects as fully as possible, and also to minimize magnetic irreversibility. To ascertain in a controlled manner the effects of electronic scattering, specific doping studies were conducted, as described below.

Single crystals of $\text{YNi}_2\text{B}_2\text{C}$, $\text{LuNi}_2\text{B}_2\text{C}$, and $\text{Lu}(\text{Ni}_{1-x}\text{Co}_x)_2\text{B}_2\text{C}$ were grown out of Ni_2B or $(\text{Ni}_{1-x}\text{Co}_x)_2\text{B}$ flux in a manner similar to the growth of other borocarbide crystals. As discussed in Ref. 8, Co doping serves as a convenient tool to move from a clean to a dirty limit. Powder x-ray-diffraction spectra taken on Y1221, Lu1221, and Lu(Ni-Co)1221 indicate that there were no detectable second phases present. Residual resistance ratios (RRRs) of pure Lu1221 and Y1221 were close to or higher than $\text{RRR}=25$.

NbSe_2 crystals were grown via iodine vapor transport technique (Ref. 9) and had $T_c\approx 7.1$ K and the residual resistivity ratio $\text{RRR}\approx 40$. MgB_2 single crystals of submillimeter sizes were grown by a high-pressure technique as described in Ref. 10. Single-crystal x-ray-diffraction measurements on MgB_2 crystals grown in similar conditions reveal no second phases present.

A single crystal of V_3Si was grown using a Bridgeman method, in which a floating zone was created by rf induction heating.¹⁹ The samples for investigation were cut by a wire saw and oriented using Laue method. Samples had a typical dimension of $2\times 2\times 4$ mm. The crystal is a “clean” superconductor, as evidenced by weak electron scattering with $\text{RRR}\approx 30$ and the fact that the mixed-state magnetization exhibits very little irreversibility (weak pinning of vortices) under the conditions of the study. Furthermore, small-angle neutron-diffraction studies on a “sister” crystal cut from the same V_3Si boule revealed the presence of sharp, very well-defined flux-line lattice reflections.¹¹

B. Magnetic measurements

The magnetization measurements were performed by using several Quantum Design MPMS systems. In a typical experiment, a full $M(H)$ loop was recorded and only its reversible part, above the irreversibility field, H_{irr} , was used for the analysis. H_{irr} was determined as a field where ascending and descending branches coincided or were sufficiently close (a weak hysteresis).

The procedure is demonstrated in Fig. 1. The main frame shows raw data with a clear range of reversible behavior above H_{irr} indicated by an arrow. The left inset shows the expanded portion of the raw data in the vicinity of H_{c2} . A small paramagnetic background (from the sample, the sample holder and perhaps residual flux on the crystal surface) is clearly seen as a linear-in- H contribution. After this contribution is subtracted, we obtain the superconducting diamagnetic signal shown in the right inset. The H_{c2} is indicated by an arrow. Superconducting transition temperature was measured in a small ($H=10$ Oe) applied field. In large fields of our interest, demagnetization effects are weak; in the following we do not distinguish between the applied field H and the induction B . As explained below, we do not need the sample volume in our analysis so that we can use on equal footing field dependencies of the magnetic moment (in *emu*) or of the magnetization (in *G*); we use the notation M for both quantities.

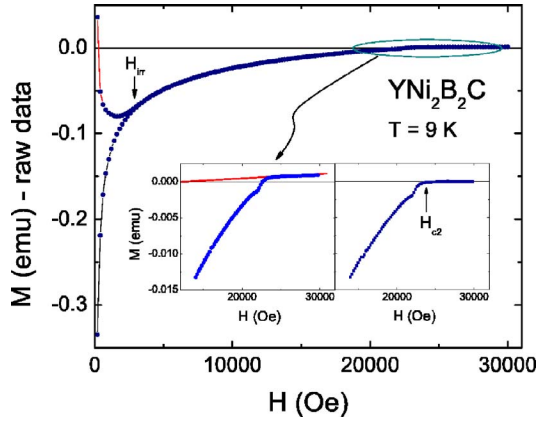


FIG. 1. (Color online) An example of $M(H)$ for $\text{YNi}_2\text{B}_2\text{C}$ at $T = 9$ K. The main plot shows both up- and down-field scans and the irreversibility field. The left inset illustrates how the normal-state paramagnetic contribution is subtracted with the result shown in the right inset.

III. MODIFIED LONDON MODEL

The standard London energy (2) gives an equilibrium magnetization that is linear in $\ln B$ in intermediate fields,

$$M = -\frac{\partial \tilde{F}}{\partial B} = -\frac{\phi_0}{32\pi^2\lambda^2} \ln \frac{\eta H_{c2}}{B}. \quad (3)$$

Hence, the standard London model requires a plot of M versus $\ln B$ to be a straight line.

A. $\text{YNi}_2\text{B}_2\text{C}$

Figure 2 shows *reversible* magnetization for a single-crystal $\text{YNi}_2\text{B}_2\text{C}$ in fields parallel to the c axis at 2, 5, 9, and 12 K. Clearly, the deviations from the London prediction increase with decreasing T ; at low temperatures $M(\ln B)$ is far from being linear.

We note that in many materials with $\kappa \gg 1$, it is difficult to distinguish between a narrow Abrikosov domain near H_{c2}

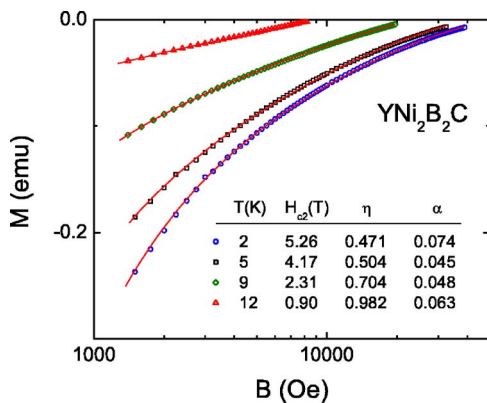


FIG. 2. (Color online) The magnetization $M(\ln B)$ for $\text{YNi}_2\text{B}_2\text{C}$ at $T = 2, 5, 9,$ and 12 K. The upper critical fields H_{c2} are the positions of kinks in $M(\ln B)$ not shown in the figure. The solid curves are obtained by fitting the data to Eq. (4) with the fitting parameters M_0 (shown in the inset of Fig. 3), η , and α .

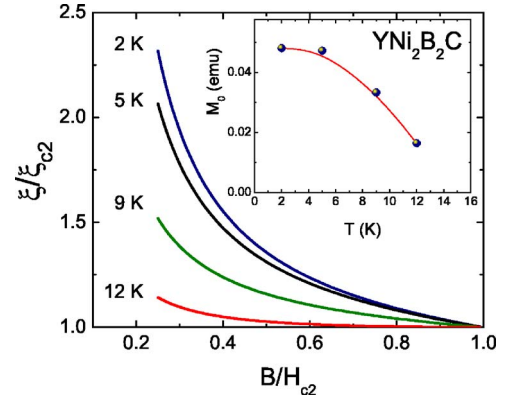


FIG. 3. (Color online) $\xi(B)$ extracted from the data of Fig. 2 for $\text{YNi}_2\text{B}_2\text{C}$ with the help of Eq. (8). The inset shows $M_0(T)$ extracted from the fits of Fig. 2.

with $M \propto (H_{c2} - B)$ and a broad London domain where the magnetization depends on the field in a slow, nearly logarithmic manner. For this reason the Abrikosov part of $M(B)$ is sometimes discarded altogether; this amounts to setting $\eta = 1$ in Eq. (3).¹² Of course, this cannot be done for materials with $\kappa \sim 1$. We will follow this simplification in our analysis and indicate the cases when this cannot be done.

To formally account for deviations of the data from the behavior prescribed by the standard London formula, we add to expression (3) two additional terms: const/B (to correct for the low-field behavior) and $\text{const} B$ (to account for the high-field curvature). These are, perhaps, the simplest possible modifications one can think about.¹³ A restriction upon the constants is provided by a requirement that $M(H_{c2}) = 0$. Hence

$$M = -M_0 \left[\ln \frac{\eta H_{c2}}{B} + \alpha \frac{H_{c2}}{B} - (\ln \eta + \alpha) \frac{B}{H_{c2}} \right], \quad (4)$$

where $M_0 = \phi_0 / 32\pi^2\lambda^2$. Certainly, the form (4) is not the only possibility for representing the available data. Other forms were suggested in the literature^{14–17} based on different theories and assumptions.¹⁸ We stress that the expression (4) is just an empirical formula to represent the data. We choose it because of its simplicity, and because—as is demonstrated below—it is sufficiently flexible to represent the magnetization data in a host of materials with very different physical properties.

The solid lines in Fig. 2 are the data fits to Eq. (4). The value of the upper critical field for each T is read directly from the raw data as explained in Fig. 1. We are left with three fit parameters M_0 , η , and α . Two of these are shown in the table of Fig. 2. The inset in Fig. 3 shows that the T dependence of $M_0 \propto 1/\lambda^2$ is qualitatively consistent with the behavior of the superfluid density $\propto \lambda^{-2}$. The quality of the fits is good; hence, the empirical form (4) can be used to represent the data reasonably accurately.

Examining possible modifications of the London model to account for the deviations of $M(\ln B)$ of Fig. 2 from linear behavior, one should bear in mind the difference between the roles of two fundamental lengths, λ and ξ , within the London

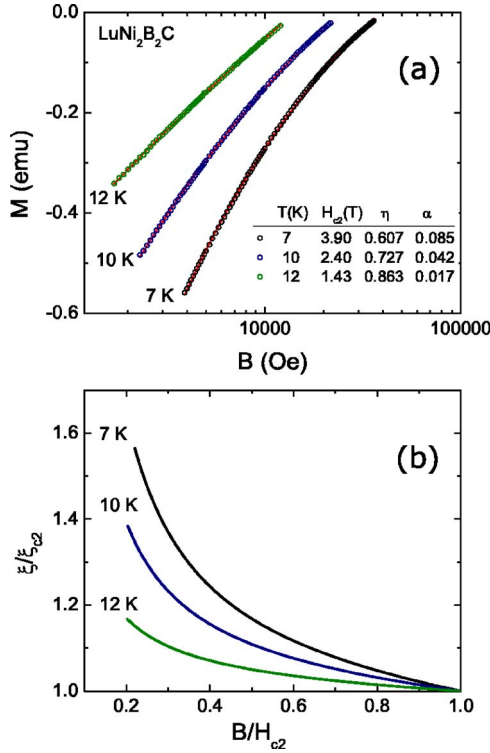


FIG. 4. (Color online) (a) $M(B)$ for $\text{LuNi}_2\text{B}_2\text{C}$ for $T=7, 10,$ and 12 K. (b) $\xi(B)$ corresponding to the graphs of the upper panel.

theory. The length λ enters Eq. (1), which is the basis of the whole approach. On the other hand, the length ξ is absent in the London equation and enters the energy expression as an uncertain cutoff used to mend the inherent shortcoming of the London model. Therefore, considering possible modifications of this model, one still has some freedom—however limited—in working with ξ , unlike the case of λ .

Comparing the data of Fig. 2 with predictions of the standard London model one wonders why the model, which describes correctly the field of vortices away from their cores, fails badly at low temperatures. From the point of view of a consistent London description, the only suspicious point in deriving the free energy (2) and the corresponding magnetization (3) is the cutoff employed, which generates the term $\ln(H_{c2}/B)$.

B. London model modified to accommodate $\xi(B)$

Hence, we write the free energy in the form

$$\tilde{F} = \frac{\phi_0 B}{32\pi^2 \lambda^2} \ln \frac{e \eta \tilde{H}(B)}{B}, \quad \tilde{H} = \frac{\phi_0}{2\pi \xi^2(B)}, \quad (5)$$

where $\xi(B)$ is the *field-dependent cutoff* (the core size). Clearly, $\xi(H_{c2})$ is the standard coherence length associated with H_{c2} , so that $\tilde{H}(H_{c2})=H_{c2}$. Then, evaluating $M=-\partial\tilde{F}/\partial B$, we obtain

$$M = -\frac{\phi_0}{32\pi^2 \lambda^2} \left(\ln \frac{\eta \tilde{H}}{B} + \frac{B}{\tilde{H}} \frac{d\tilde{H}}{dB} \right). \quad (6)$$

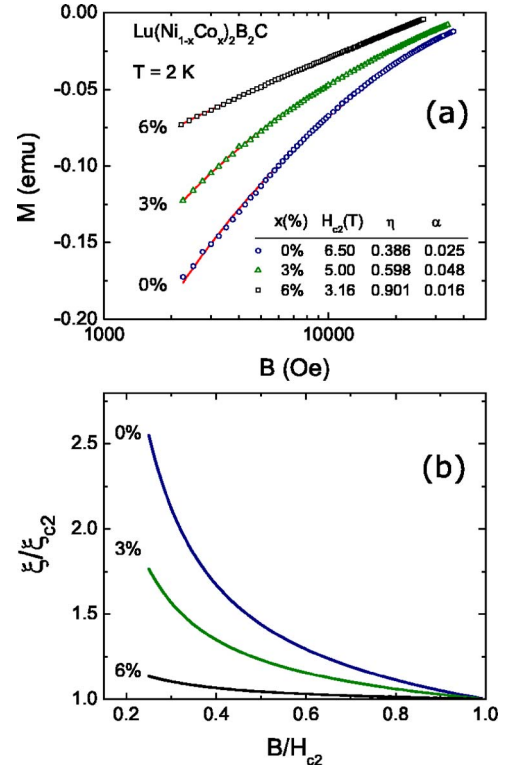


FIG. 5. (Color online) (a) $M(B)$ for $\text{Lu}(\text{Ni}_{1-x}\text{Co}_x)_2\text{B}_2\text{C}$ with $x=0, 3,$ and 6% . (b) $\xi(B)$ corresponding to the graphs of the upper panel.

The idea of the following manipulation is to find a field \tilde{H} that generates the form (4), or in other words, that represents the experimental data. After equating Eqs. (6) and (4), one can solve a linear differential equation for $\tilde{H}(B)$ with the boundary condition $\tilde{H}(H_{c2})=H_{c2}$. The result in terms of $\tilde{h}=\tilde{H}/H_{c2}$ and $b=B/H_{c2}$ reads

$$\ln \tilde{h} = \frac{\alpha}{b} \ln b + \frac{(\ln \eta + \alpha)(1 - b^2)}{2b}. \quad (7)$$

This corresponds to the normalized cutoff distance (the core radius)

$$\xi^*(B) = \frac{\xi(B)}{\xi_{c2}} = b^{-\alpha/2b} \exp \frac{(\ln \eta + \alpha)(b^2 - 1)}{4b}. \quad (8)$$

It is readily shown that the slope of $\xi^*(b)$ at H_{c2} is determined by the parameter η ,

$$\left. \frac{d\xi^*}{db} \right|_{b=1} = \frac{1}{2} \ln \eta. \quad (9)$$

Hence, when the field decreases from H_{c2} , $\xi(B)$ decreases for $\eta > 1$ and increases for $\eta < 1$.

Using Eq. (8), we can calculate the normalized cutoff $\xi^*(b)$ responsible for deviations of $M(B, T)$ from the standard London behavior for $\text{YNi}_2\text{B}_2\text{C}$ shown in Fig. 2 since we have η and α representing these data sets [note that M_0 does not enter Eq. (8)]. The curves $\xi^*(b)$ for $T=2, 5, 9,$ and 12 K calculated with Eq. (8) are shown in Fig. 3.

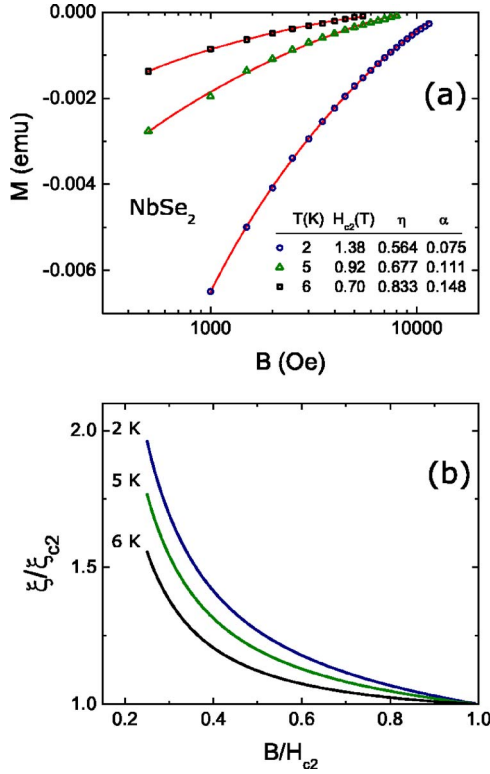


FIG. 6. (Color online) (a) $M(B)$ for NbSe_2 . (b) $\xi(B)$ corresponding to the graphs of the upper panel.

It is worth observing that $\xi(B)$ so obtained is qualitatively similar to the B dependence of the core size seen in μSR experiments.² Moreover, it is argued in Ref. 6 that the field dependence of ξ should weaken with increasing temperature in accord with Fig. 3.

Another point to make is that only a moderate variation of ξ is needed to account for strong deviations from the linear $M(\ln B)$. For example, at 2 K, ξ changes only by a factor of 2 over most of the mixed-state field domain. Since the cutoff enters the energy (5) under the log sign, it might be surprising that such a difference suffices to cause a drastic deviation of the 2 K curve in Fig. 2 from a straight line. The puzzle is resolved if one observes that the field dependence of ξ translates to *nonlogarithmic* corrections to the standard London magnetization, see Eq. (6).

The same analysis has been applied to the magnetization data for a crystal of $\text{LuNi}_2\text{B}_2\text{C}$ (whose crystal structure and superconductive properties are similar to $\text{YNi}_2\text{B}_2\text{C}$), yielding similar results as shown in Fig. 4.

C. $\text{Lu}(\text{Ni}_{1-x}\text{Co}_x)_2\text{B}_2\text{C}$

As mentioned, Ref. 6 argues that the field dependence of the core size is weakened by increasing temperature and scattering. In order to study the scattering dependence of $\xi(B)$, we turn to a series of crystals $\text{Lu}(\text{Ni}_{1-x}\text{Co}_x)_2\text{B}_2\text{C}$ in which the mean-free path is progressively reduced by increasing the Co content.⁸

In the upper panel of Fig. 5, $M(B)$ is shown for $x=0, 3,$ and 6% (for which H_{c2} has been independently measured) at

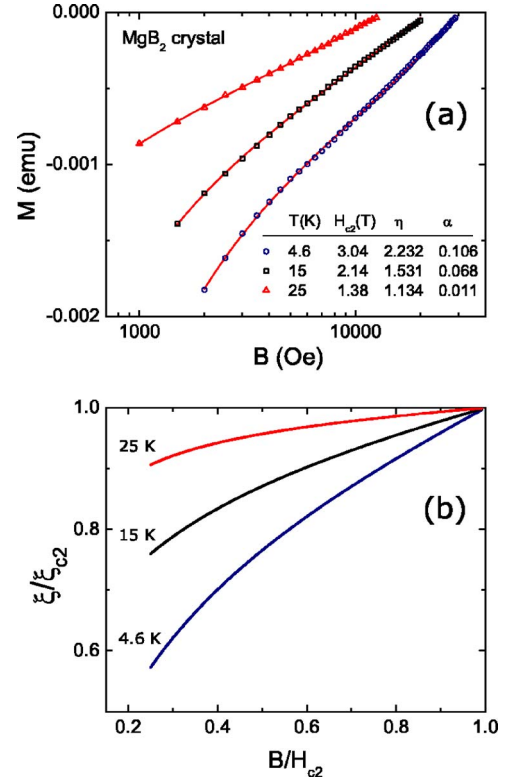


FIG. 7. (Color online) (a) MgB_2 , $T=4.6, 15,$ and 25 K. (b) Corresponding $\xi(B)$.

the same temperature of 2 K. The fit parameters η and α are also shown and the calculated field-dependent core sizes are given in the lower panel.

We note that for 6% Co, the ratio of the zero- T coherence length to the mean-free path has been estimated in Ref. 8 as exceeding ten, which places this sample close to the dirty limit. The core size for this crystal is seen to vary only by about 10%, which is in accord with the theoretical finding that field dependence of ξ disappears in the dirty limit.^{5,6}

D. NbSe_2

The superconducting anisotropy of this material is stronger than in borocarbides discussed above. As is seen in Fig. 6, deviations of $M(\ln B)$ from the standard London linearity are profound along with the corresponding field dependence of ξ .

E. MgB_2

The upper panel of Fig. 7 shows $M(\ln B)$ in fields parallel to the c axis of a single-crystal MgB_2 . One readily sees a qualitative difference from the preceding examples: the curvature of $M(\ln B)$ for $T=4.6$ K being negative in low fields becomes positive in large fields. Still, we can fit well the data for all T 's to the form of Eq. (4) with parameters η and α given in the table.

The most interesting feature is that the obtained values of η exceed unity. According to Eq. (9) this means that starting from H_{c2} , ξ decreases with decreasing field. This is shown in

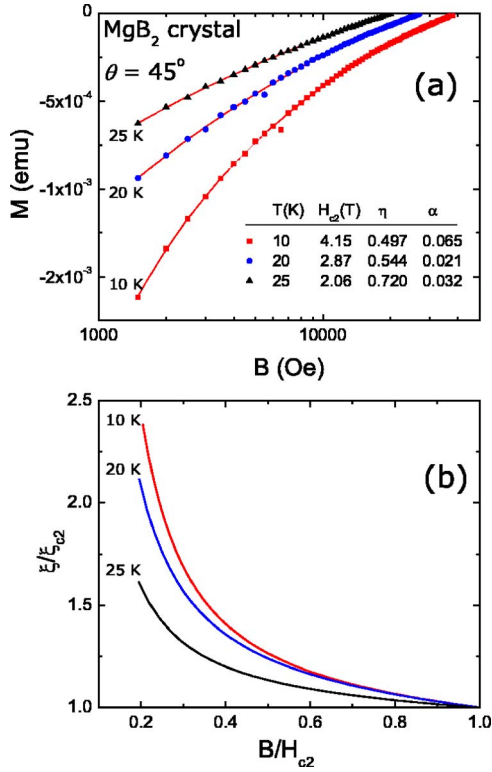


FIG. 8. (Color online) (a) Magnetization of the MgB_2 crystal in applied field at 45° to the c axis. (b) Corresponding coherence length. Note the difference in the behavior of $\xi^c(b)$ from the case of the field along c of Fig. 7.

the lower panel of Fig. 7. We attribute this unusual behavior to the two-gap nature of this material: the small gap on the π sheet of the Fermi surface opens up in decreasing fields thus causing a decrease of ξ .

If indeed the unusual behavior of $\xi(B)$ for MgB_2 is due to suppression of the small gap in fields of few kG for $H\parallel c$, and if the suppression field is *isotropic*, then by going to other field orientation away from the c axis with a higher H_{c2} , we can push the effect of the small gap out of the high-field domain of our interest. To check this hypothesis we acquired the data for the applied field at 45° to the c axis where $H_{c2}(0)$ is accessible with our equipment. Figure 8 shows the result similar to that for Y and Lu-based borocarbides. This suggests that, e.g., for $T=10$ K, in the field domain examined (from $H_{c2}=4.15$ T down to about 0.4 T or $b\approx 0.1$) the small gap is not yet fully formed.

Of course, this interpretation is much too simple because for other than $H\parallel c$ orientation the strong anisotropy of ξ should be taken into account, the subject of our future work. It should also be noted that the macroscopic phenomenology of magnetic properties of MgB_2 is still debated. Despite the two-band nature of this material, within the London approach, we employ *one* penetration depth λ and *one* cutoff length ξ when describing the vortex lattice in reciprocal space. Judging by literature, this point of view is not universally shared by the entire MgB_2 community.

F. V_3Si

For this study, the magnetic field was applied along the crystalline [110] axis. Given the slope $dH_{c2}/dT=19.4$ T/K

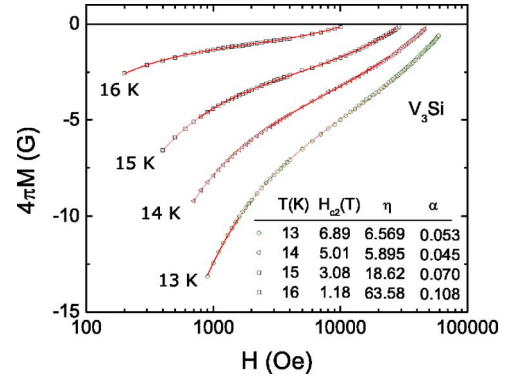


FIG. 9. (Color online) Magnetization of the V_3Si single crystal at $T=13, 14, 15$, and 16 K.

and $T_c=16.6$ K, it is likely that the low-temperature upper critical field of this material exceeds 20 T; no direct measurements of H_{c2} were conducted in this field range. One might treat H_{c2} as an extra fitting parameter to be extracted from the data on $M(B)$. However, the numerical procedure of extracting both H_{c2} and η from the magnetization data is unstable because their product enters the formulas we use. For this reason, we consider here only $M(B)$ for $T>13$ K for which H_{c2} was measured.

It is worth noting that Eq. (4) is good enough even for a quite unusual shape of $M(\ln B)$ in this material: the curvature of $M(\ln B)$ changes sign in all data we have examined. With the help of Eq. (4) we readily find that the inflection point is at $b_i=\sqrt{\alpha/(\alpha+\ln \eta)}$. With the parameters from the table in Fig. 9 we obtain $b_i\approx 0.16$, for all temperatures.²⁰ Therefore, the curves $M(\ln B)$ are concave for $b<b_i\approx 0.16$, i.e., at fields hardly in the domain of applicability of our high-field model. On the other side of the inflection point where the curves $M(\ln B)$ are convex, we may be dealing with the Abrikosov domain where M is linear in $H_{c2}-B$; it is easy to see then that $M(\ln B)$ should be convex.²¹ Application of the London approach in this domain cannot be justified. Therefore, there is no point in trying to extract $\xi(B)$ from the data on V_3Si . (Formally, since all η 's in the table of Fig. 9 exceed unity, this extraction would have given $\xi(B)$ decreasing with decreasing field, which would have contradicted the μSR data of Ref. 22.)

Finally, it is worth noting that further measurements on another crystal from the same high-quality boule, but with the magnetic field applied along the threefold symmetric [111] crystalline axis, yielded similar results with an inflection point at intermediate fields.

IV. DISCUSSION

The main point of this work is to argue that the field dependence of the core size is a generic low-temperature property of all sufficiently clean superconductors. Incorporating this dependence in the London approach broadens considerably its applicability for describing macroscopic reversible magnetic properties. Still, the empirical approach adopted here lacks microscopic justification. If proven cor-

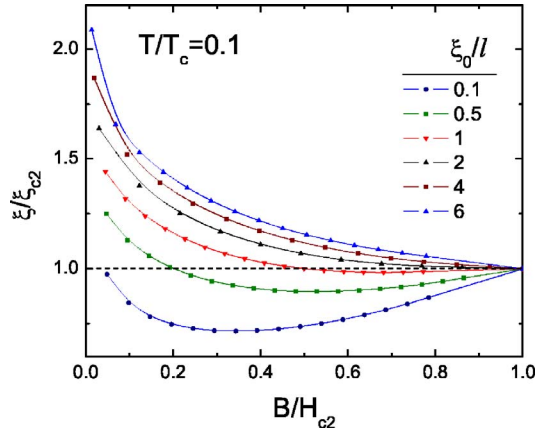


FIG. 10. (Color online) The field dependence of ξ calculated microscopically for $T/T_c=0.1$ and for a few scattering parameters ξ_0/ℓ where ξ_0 is zero- T BCS coherence length and ℓ is the mean-free path for scattering on nonmagnetic impurities.

rect, the modified London scheme calls for revisiting many results obtained within the standard London model in which the field-independent core size or the cutoff are involved. Field dependencies of the flux-flow resistivity, of the specific heat in the mixed state, or the core pinning are some examples.

One can foresee a number of difficulties in trying to develop such a justification. The cutoff size we extract from $M(B)$ data is not necessarily the same as the core size defined as being proportional to the slope of the order parameter at the vortex axis: approaching the core from the outside to determine the cutoff we may have a different result than when examining the core structure starting from the core center. Having this in mind, it is not surprising that the microscopic calculations of $\rho_c \propto (d\Delta/dr|_{r \rightarrow 0})^{-1}$ in Ref. 7 do not agree in detail with our empirical results (to our knowledge, this is the only calculation of this sort that has been tried to date). Figure 10 shows the output of this calculation normalized in the manner of this paper for a model isotropic material at $T=0.1T_c$ and for a few values of the scattering parameter ξ_0/ℓ ($\xi_0 = \hbar v_F / \pi \Delta(0)$ is the zero- T BCS coherence length and ℓ is the mean-free path for the nonmagnetic scattering). We note that while most of the curves generated are qualitatively similar to what we extract from the magnetization data, this calculation does not confirm our assertion about weakening of the field dependence of the core size with increasing scattering.

A different approach to evaluation of the core size is chosen in Ref. 6: it is argued on physical grounds that since $\Delta \rightarrow 0$ at the vortex center and the field is practically uniform within the core for $\kappa \gg 1$, one can use Helfand-Werthamer's linearization technique²³ for calculation of H_{c2} and also for the core size in the high-field mixed state. Within this approach, the order parameter near the vortex center satisfies a linear equation $-\xi^2 \nabla^2 \Delta = \Delta$, where $\nabla = \nabla + 2\pi \mathbf{r} \mathbf{A} / \phi_0$ and ξ is found solving the basic BCS self-consistency equation. This produces $\xi(T, \ell; B)$ in qualitative agreement with what we extract from the magnetization data in this work (for all cases other than $V_3\text{Si}$ and MgB_2 in the field along the c axis); in particular, the analytical field dependence of ξ obtained in

this way disappears when $T \rightarrow T_c$ or $\ell / \xi_0 \rightarrow 0$.

In our view, the question still remains: Which of these two theoretical approaches, Ref. 7 or Ref. 6, describes better various data on $\xi(B)$? An important role in resolving the question belongs to experimental studies of how the field dependence of the core size affects other physical properties of the mixed state.

A. Flux-flow resistivity

As an example of such a cross examination we took data on the flux-flow resistivity ρ_f from measurements of the microwave surface impedance of $\text{YNi}_2\text{B}_2\text{C}$.²⁴ The data show large deviations of the measured ρ_f from the Bardeen-Stephen linear field dependence, $\rho_f = \rho_n B / H_{c2}$. This formula is obtained assuming a field-independent core size $\xi = \xi_{c2} = \sqrt{\phi_0 / 2\pi H_{c2}}$. Clearly, if ξ does depend on the field, one has

$$\frac{\rho_f}{\rho_n} = B \frac{2\pi \xi^2(B)}{\phi_0} = \frac{B}{H_{c2}} \frac{\xi^2(B)}{\xi_{c2}^2} = b \xi^{*2}(b). \quad (10)$$

Hence, for each data set $\rho_f(B)$, we can extract

$$\frac{\xi(B)}{\xi_{c2}} = \sqrt{\frac{\rho_f(B)}{\rho_n b}}. \quad (11)$$

In other words, we can delegate deviations from $\rho_f \propto B$ to the field dependence of ξ and see whether or not the obtained $\xi(B)$ agrees with that extracted from magnetization data.

Utilizing the flux-flow resistivity data of Fig. 3 of Ref. 24 and applying Eq. (11), we obtain the result shown in the panel (a) of Fig. 11. Comparing it with our Fig. 3 for the same material, we obtain reasonable agreement, notwithstanding the usage of different samples in these two experiments.

As another example, two selections of data for $\text{Y}(\text{Ni}_{1-x}\text{Pt}_x)_2\text{B}_2\text{C}$ from Fig. 3 of Ref. 25 were used to calculate $\xi(B)/\xi_{c2}$, as shown in Fig. 11(b). We see that in addition to the expected decrease with field, $\xi(B)$ is suppressed by increasing scattering (i.e., increasing impurity content of Pt) again in accord with the examples discussed above.

Panel (c) of Fig. 11 shows the result of the same exercise with a d -wave material (an overdoped crystal of Bi-2201).²⁶ This example supports the idea that the field dependence of the London cutoff is a generic feature of type-II superconductors with no direct relation to the order-parameter symmetry.

The last panel of Fig. 11 presents the cutoff $\xi(b)/\xi_{c2}$ for two field orientations of MgB_2 extracted from the flux-flow resistivity data of Ref. 27, again using Eq. (11). For the field along ab , both $M(B)$ and $\rho_f(B)$ data yield qualitatively similar results. This, however, is not the case for the field along c as evident by comparing Figs. 7 and 11(d). Thus it appears that for the two-gap MgB_2 with its greater complexity, the simple scheme of incorporating a field-dependent cutoff to the London model does not work for all field orientations.

B. On nonlocality

Deviations in $M(\ln B)$ from the standard London linear behavior have been thought to come from the effects of the

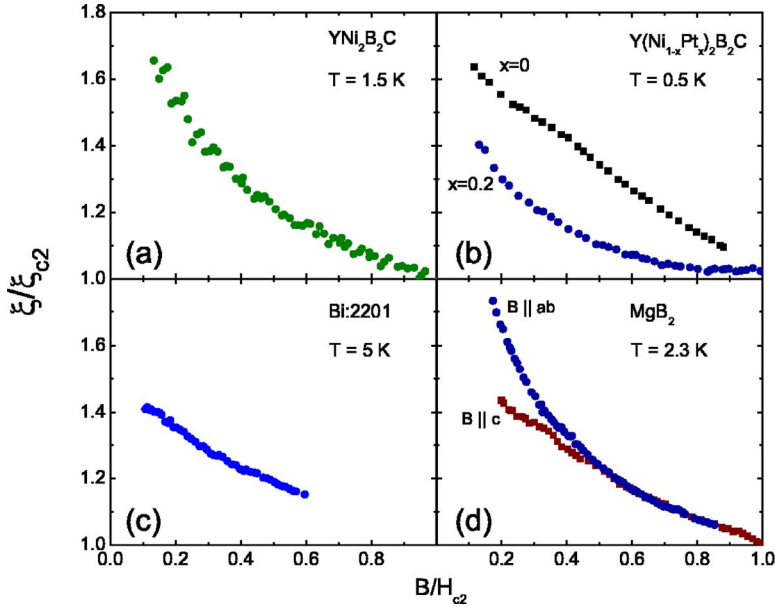


FIG. 11. (Color online) $\xi(b)/\xi_{c2}$ vs $b=H/H_{c2}$ extracted from the flux-flow resistivity data as explained in the text.

nonlocal relation between current and the vector potential inherent for superconductors.¹⁷ The nonlocal corrections to London theory turned out to be an effective tool in describing evolution and transitions in vortex lattice structures.³⁰ However, it is difficult at this stage to sort out what part of the deviations of M from linear-in- $\ln B$ behavior arises solely from the core-size field dependence and what part should be relegated to the nonlocality. In particular, the difficulty comes from analogous weakening of the two effects with increasing temperature and scattering strength. Looking back to the overall satisfactory data analysis of $M(\ln B)$ for $\text{Lu}(\text{Ni}_{1-x}\text{Co}_x)_2\text{B}_2\text{C}$ of Ref. 29 based on nonlocal effects, we note that the analysis produced an excessively rapid reduction of the “nonlocality range” with temperature for samples with elevated impurity content. We have to conclude that more high-precision experimental results are needed before a conclusive judgment is made on the relative importance of contributions to $M(B)$ due to the nonlocality and to the field dependence of the core size.

C. Why $\lambda(B)$ should be used with caution within London theory

As mentioned above, the basic London equation (1) along with the energy expression (2) for intermediate fields [or Eq. (5) with an unspecified cutoff] imply that the London penetration depth λ is a temperature-dependent *constant* in a homogeneous material. Assuming a field dependent λ would have changed the London equation (1) *per se*: the quantity $\lambda^2(h)$ cannot be taken out of differentiation operators. As a result, the Fourier components of the solution $h(\mathbf{k})$ for a single vortex would have been different from $\phi_0/(1+\lambda^2k^2)$ and the energy (2) would have been different as well. Therefore, unlike the case of the cutoff ξ , relaxing the requirement of a constant λ causes basic changes in the London approach and therefore should not be taken lightly. It is also worth recalling that a constant λ is derived from the microscopic Bardeen–Cooper–Schrieffer theory (as $\mathbf{k} \rightarrow 0$ limit of the ker-

nel in the nonlocal connection between the persistent current and the vector potential). To our knowledge, there is no microscopic justification for a field dependent λ (in nonmagnetic superconductors). In other words, the London theory is rigid with respect to a constancy of λ , unlike the case of ξ .

Yet, quite often, analyzing data with the help of the London model (i.e., starting with a constant λ) it is concluded that λ should be field dependent. Numerous examples are found in the literature on μSR (see, e.g., Ref. 2) and in many recent publications on MgB_2 .^{28,31–33} An “operational” justification implied for this apparent contradiction usually goes like this: of course, the field distribution for a single vortex is described by Eq. (1) with a constant λ . However, in the mixed state the average order parameter is suppressed by overlapping vortex fields, and therefore, the “macroscopic” Λ (\neq to λ calculated for $H \rightarrow 0$) should enter the free energy Eq. (2). This macroscopic parameter may depend on the average magnetic field B .

The inconsistency of such an argument is exposed if one considers the clean limit at zero temperature. In this case the London λ does not depend on the order parameter (in fact, it depends only on the total electron density), so that the mixed-state order-parameter suppression cannot be referred to as a general justification for employing $\Lambda(B)$.

D. On the superfluid density

The quantity $\lambda^2(0)/\lambda^2(T)$ is often taken as a measure of the superfluid density n_s . This assignment has unambiguous justification only for isotropic superconductors (see, e.g., Ref. 34) and when $\lambda(T)$ is defined as the penetration depth of a small magnetic field (strictly speaking in the limit $H \rightarrow 0$). One of the attractive features of the standard London theory is that one can extract $1/\lambda^2(T)$ directly from the magnetization (3) by measuring the constant slope $dM/d(\ln B)$ for each temperature. This way of determining the superfluid density n_s rests, therefore, upon whether or not the standard London model for M is valid. As we have seen in a number of ex-

amples above, this is quite often not the case.

Perhaps the best example of the futility of extracting n_s from magnetization data is provided by the data for V_3Si . As is seen in Fig. 9, e.g., for $T=14$ K, the slope $dM/d(\ln B)$ decreases with the field increasing up to ~ 1 T, but it grows with further field increase toward H_{c2} . If one takes literally the proportionality between n_s and the slope $dM/d(\ln B)$, one should conclude that the field suppresses the “superfluid density” as long as B is under ≈ 1 T but for $B > 1$ T, n_s is enhanced by increasing field.

Hence, extracting any quantitative information about the superfluid density or the penetration depth from the magnetization data with the help of the *standard* London model should be taken “with a grain of salt” at best even for such “simple” materials as V_3Si , not to mention MgB_2 in which the different field behavior of the two gaps further complicates the matter.^{28,32,33}

To summarize, the field dependence of the core size $\xi(B)$ has been incorporated in the London model to describe intermediate-field reversible magnetization $M(B, T)$ for materials with large κ . The dependence $\xi(B)$ is directly related to deviations in $M(\ln B)$ from linear behavior prescribed by the standard London model. A method to extract $\xi(B)$ from

the magnetization data is proposed. For most materials examined, $\xi(B)$ so obtained decreases with increasing field; the dependence becomes weaker with increasing temperature or with strengthening the nonmagnetic scattering, in qualitative agreement with theoretical predictions and with existing μ SR, SANS, and flux-flow resistivity data. The method, however, fails when applied to MgB_2 and—surprisingly—to V_3Si , the subject for a separate discussion.

ACKNOWLEDGMENTS

The authors thank Morten Eskildsen for useful discussions and for sharing SANS data on $CeCoIn_5$ before publication. They also thank P. Gammel for providing $NbSe_2$ crystals. Ames Laboratory is operated for U.S. DOE by the Iowa State University under Contract No. W-7405-Eng-82. Research at ORNL was sponsored by the Division of Materials Sciences and Engineering, Office of Basic Energy Sciences, U.S. Department of Energy, under Contract No. DE-AC05-00OR22725 with Oak Ridge National Laboratory, managed and operated by UT-Battelle, LLC. R.P. acknowledges support from NSF Grant No. DMR-05-53285 and from the Alfred P. Sloan Foundation.

*Corresponding author. Electronic address: prozorov@ameslab.gov

¹P. DeGennes, *Superconductivity of Metals and Alloys* (Addison-Wesley, New York, 1989).

²J. E. Sonier, *J. Phys.: Condens. Matter* **16**, 4499 (2004).

³In μ SR experiments, the field-dependent muons decay is utilized to map the field distribution in the mixed state. One of the ways to estimate the core size is to extract the distribution of microscopic supercurrents and to define the core boundary as a place where the current reaches maximum. Another way is to fit the experimental field distribution to the distribution obtained within the London model in which ξ enters via a somewhat uncertain cutoff (see details in Ref. 2). Both methods yield qualitatively similar results.

⁴L. DeBeer-Schmitt, C. D. Dewhurst, B. W. Hoogenboom, C. Petrovic, and M. R. Eskildsen, *Phys. Rev. Lett.* **97**, 127001 (2006).

⁵V. G. Kogan, *Phys. Rev. B* **32**, 139 (1985); V. G. Kogan and N. Nakagawa, *ibid.* **35**, 1700 (1987).

⁶V. G. Kogan and N. V. Zhelezina, *Phys. Rev. B* **71**, 134505 (2005).

⁷P. Miranović, M. Ichioka, and K. Machida, *Phys. Rev. B* **70**, 104510 (2004).

⁸K. O. Cheon, I. R. Fisher, V. G. Kogan, P. C. Canfield, P. Miranovic, and P. L. Gammel, *Phys. Rev. B* **58**, 6463 (1998).

⁹C. S. Oglesby, E. Bucher, C. Kloc, and H. Hohl, *J. Cryst. Growth* **137**, 289 (1994).

¹⁰J. Karpinski, M. Angst, J. Jun, S. M. Kazakov, R. Puzniak, A. Wisniewski, J. Roos, H. Keller, A. Perucchi, L. Degiorgi, M. R. Eskildsen, P. Bordet, L. Vinnikov, and A. Mironov, *Supercond. Sci. Technol.* **16**, 221 (2003).

¹¹M. Yethiraj, D. K. Christen, D. McK. Paul, P. Miranovic, and J. R. Thompson, *Phys. Rev. Lett.* **82**, 5112 (1999).

¹²M. Tinkham, *Introduction to Superconductivity* (McGraw-Hill, New York, 1996), Sec. 5.3.2.

¹³Eq. (4) is in fact a general expansion of a function singular as $b=B/H_{c2} \rightarrow 0$: $c_1/b+c_2 \ln b+c_3+c_4b+\dots$.

¹⁴E. H. Brandt, *J. Low Temp. Phys.* **26**, 709 (1977).

¹⁵Z. Hao, J. R. Clem, M. W. McElfresh, L. Civale, A. P. Malozemoff, and F. Holtzberg, *Phys. Rev. B* **43**, 2844 (1991).

¹⁶A. E. Koshelev, *Phys. Rev. B* **50**, 506 (1994).

¹⁷V. G. Kogan, A. Gurevich, J. H. Cho, D. C. Johnston, Ming Xu, J. R. Thompson, and A. Martynovich, *Phys. Rev. B* **54**, 12386 (1996).

¹⁸The Ginzburg-Landau (GL) approach for treating the mixed-state magnetization can be extended to low temperatures only for special situations like gapless superconductivity. Moreover, even close to T_c where GL works, there is no closed GL expression for the magnetization away of H_{c2} . On the other hand, the magnetization data near T_c are noisy, and comparison with experiment in this domain would be difficult if not impossible even if the GL theory would have made a prediction for $\xi(H)$.

¹⁹D. K. Christen, H. R. Kerchner, S. T. Secula, and Y. K. Chang, *Proceedings of the 17th International Conference on Low Temperature Physics, Karlsruhe, Germany, 1984*, edited by U. Eckern, A. Schmid, W. Weber, and H. Wuehl (Elsevier, Amsterdam, 1984), p. 1035.

²⁰This suggests a possibility of a certain scaling procedure as a result of which all $M(\ln b)$ of Fig. 9 nearly collapse to a single curve. We will not dwell on this matter, since the physical meaning of such a scaling is still unclear.

²¹One can calculate the linear slope $dM/dB|_{B \rightarrow H_{c2}}$ using Eq. (4) to obtain $(1+2\alpha+\ln \eta)/16\pi\kappa^2$. The Abrikosov slope is $\approx 1/8\pi\kappa^2\beta_A$ with $\beta_A=1.16$ for a triangular lattice at $T \rightarrow T_c$. It is now easy to see that Eq. (4) with parameters η and α from the

- table in Fig. 9 for $T=16$ K (which is close to $T_c \approx 16.8$ K) gives the slope of the same order as that calculated according to Abrikosov. This suggests that in V_3Si the Abrikosov domain might be very broad. We note that if ρ_c would behave as $\approx \xi_{c2}/\sqrt{b}$ in a broad domain under H_{c2} , the intervortex distance would have been on the order of ρ_c ; in other words, one would expect Abrikosov's linear $M(B)$ in this domain. This speculation is worth experimental examination.
- ²²J. E. Sonier, F. D. Callaghan, R. I. Miller, E. Boaknin, L. Taillefer, R. F. Kiefl, J. H. Brewer, K. F. Poon, and J. D. Brewer, *Phys. Rev. Lett.* **93**, 017002 (2004).
- ²³E. H. Helfand, and N. R. Werthamer, *Phys. Rev.* **147**, 288 (1966).
- ²⁴K. Izawa, A. Shibata, Yuji Matsuda, Y. Kato, H. Takeya, K. Hirata, C. J. van der Beek, and M. Konczykowski, *Phys. Rev. Lett.* **86**, 1327 (2001).
- ²⁵K. Takaki, A. Koizumi, T. Hanaguri, M. Nohara, H. Takagi, K. Kitazawa, Y. Kato, Y. Tsuchiya, H. Kitano, and A. Maeda, *Phys. Rev. B* **66**, 184511 (2002).
- ²⁶Y. Matsuda, A. Shibata, K. Izawa, H. Ikuta, M. Hasegawa, and Y. Kato, *Phys. Rev. B* **66**, 014527 (2002).
- ²⁷A. Shibata, M. Matsumoto, K. Izawa, Y. Matsuda, S. Lee, and S. Tajima, *Phys. Rev. B* **68**, 060501(R) (2003).
- ²⁸M. Angst, D. Di Castro, D. G. Eshchenko, R. Khasanov, S. Kohout, I. M. Savic, A. Shengelaya, S. L. Budko, P. C. Canfield, J. Jun, J. Karpinski, S. M. Kazakov, R. A. Ribeiro, and H. Keller, *Phys. Rev. B* **70**, 224513 (2004).
- ²⁹V. G. Kogan, S. L. Bud'ko, I. R. Fisher, and P. C. Canfield, *Phys. Rev. B* **62**, 9077 (2000).
- ³⁰V. G. Kogan, P. Miranovic, and D. McK. Paul, *Series on Directions in Condensed Matter Physics*, edited by C. A. R. Sa de Melo (World Scientific, Singapore, 1998), Vol. 13, p. 127.
- ³¹R. Cubitt, M. R. Eskildsen, C. D. Dewhurst, J. Jun, S. M. Kazakov, and J. Karpinski, *Phys. Rev. Lett.* **91**, 047002 (2003).
- ³²M. Eisterer, M. Zehetmayer, H. W. Weber, and J. Karpinski, *Phys. Rev. B* **72**, 134525 (2005).
- ³³T. Klein, L. Lyard, J. Marcus, Z. Holanova, and C. Marcenat, *Phys. Rev. B* **73**, 184513 (2006).
- ³⁴A. A. Abrikosov, *Fundamentals of the Theory of Metals* (North-Holland, New York, 1988).